Dynamics of localized structures in reaction-diffusion systems induced by delayed feedback

Svetlana V. Gurevich*
Institute for Theoretical Physics, University of Münster, Wilhelm-Klemm-Str. 9, D-48149 Münster, Germany
(Received 7 March 2013; published 31 May 2013)

We are interested in stability properties of a single localized structure in a three-component reaction-diffusion system subjected to the time-delayed feedback. We shall show that variation in the product of the delay time and the feedback strength leads to complex dynamical behavior of the system, including formation of target patterns, spontaneous motion, and spontaneous breathing as well as various complex structures, arising from combination of different oscillatory instabilities. In the case of spontaneous motion, we provide a bifurcation analysis of the delayed system and derive an order parameter equation for the position of the localized structure, explicitly describing its temporal evolution in the vicinity of the bifurcation point. This equation is a subject to a nonlinear delay differential equation, which can be transformed to the normal form of the pitchfork drift bifurcation.

DOI: 10.1103/PhysRevE.87.052922 PACS number(s): 05.45.Yv, 89.75.Fb, 02.30.Ks

I. INTRODUCTION

In the field of nonlinear dynamics, control and engineering of dynamical behavior of spatial-temporal patterns in high-dimensional nonequilibrium systems is one of the key issues of recent research [1,2]. A variety of different control methods have been developed within the last decade. A particularly quite simple and efficient scheme is time-delayed feedback [3] (also referred to as Pyragas control or time-delay autosynchronization). The method allows a noninvasive stabilization of unstable periodic orbits of dynamical systems and has been also successfully applied to a number of both theoretical and experimental high-dimensional spatially extended systems (see, e.g., [4–9]). However, the influence of the time-delayed feedback on the dynamics of complex spatial-temporal patterns is still not understood to a large extent.

Among other patterns, control of dissipative localized structures (single isolated, randomly distributed, or organized in clusters) have been of increasing interest in recent years. Self-organized localized solitary patterns have been found in very different areas of research and turned out to be of particular interest for fundamental studies as well as for applications (see, e.g., [10–12] and references thereafter). In dissipative systems, they are often referred to as dissipative solitons [10,11,13]; other frequently used terminology includes autosolitons [14], oscillons [15], as well as spots, pulses, and spikes [2,10].

In particular, traveling pulses and fronts subjected to time-delayed feedback appear in various contexts. The effect of time-delayed feedback, caused by the time interval between successive migrations of biological species, on the modeling of biological range expansions was investigated in [16,17] by means of one-dimensional hyperbolic reaction-diffusion equations and compared to experimental data. Propagating depolarization waves appearing for both migraine and stroke were studied in detail in [18–20]. In particular, the onset of pulse propagation in one spatial dimension with control by augmented transmission capability, provided either along nonlocal spatial coupling or by time-delayed feedback, was discussed. The stability of a kink in a reaction-diffusion system subjected to time-delayed feedback and a delay-induced bifurcation to moving fronts was investigated in [21].

In nonlinear optics, a model for the study of localized structures, referred to as cavity solitons, in board area vertical-cavity surface-emitted lasers subjected to time-delayed feedback was proposed in [22,23]. Properties of two-dimensional cavity solitons by means of the Swift-Hohenberg equation subjected to time-delayed feedback were studied in [24]. It was shown that when the value of the control parameter, defined as a product of the delay time and the feedback strength, exceeds some critical value, a single cavity soliton starts to move in an arbitrary direction. Moreover, an analytical formula for its velocity was derived. Recently, the influence of the delayed feedback on the stability properties of a single localized structure in the Swift-Hohenberg equation was investigated in detail [25]. In particular, it was demonstrated that variation in the same control parameter leads to complex dynamical behavior of the system, including formation of oscillons, soliton rings, or labyrinth patterns. Moreover, a bifurcation analysis of the delayed system was provided and a system of order parameter equations for the position of the localized structure as well as for its shape was derived.

In this paper, we are interested in the influence of the delayed feedback on the stability properties of a single localized structure in a three-component reaction-diffusion system with one activator and two inhibitors. In contrast to the Swift-Hohenberg model, mentioned above, the reaction-diffusion system possesses no Lyapunov functional, which makes analytical treatment much more complicated. We demonstrate that the presence of the time-delayed feedback can induce complex spatial-temporal behavior of the localized structures, including the formation of target patterns, spontaneous motion, spontaneous breathing, as well as various complex structures resulting from multimode oscillatory instabilities. We also show that using the product of the delay time and delay strength as a control parameter, one can control the instability type in a straightforward manner. In addition, in the case of spontaneous motion, we derive an order parameter equation for the position of the localized structure. The position obeys a nonlinear delay-differential equation, which can be transformed to the normal form of the pitchfork drift bifurcation.

We start with the three-component reaction-diffusion system, consisting of a FitzHugh-Nagumo core equation for an

*gurevics@uni-muenster.de

activating component $u = u(\mathbf{r},t)$, $\mathbf{r} \in \mathbb{R}^2$ and an inhibiting component $v = v(\mathbf{r},t)$, enhanced by a third equation, describing the dynamics of a second, fast diffusive inhibitor $w = w(\mathbf{r},t)$:

$$\begin{aligned} \partial_t u &= D_u \Delta u + f(u) - \kappa_3 v - \kappa_4 w + \kappa_1 \\ &\quad + \alpha [u(t) - u(t-\tau)], \\ \eta \partial_t v &= D_v \Delta v + u - v + \eta \alpha [v(t) - v(t-\tau)], \\ \theta \partial_t w &= D_w \Delta w + u - w + \theta \alpha [w(t) - w(t-\tau)]. \end{aligned} \tag{1}$$

Here, in the polynomial nonlinear function $f(u) = \lambda u - u^3$, the coefficient λ is positive. The diffusion coefficients D_u, D_v, D_w of the corresponding components are positive as well as dimensionless constants, representing the ratios of the characteristic times of both inhibitors v and w with respect to that of the activator. The coefficient κ_1 violates the inversion symmetry and has arbitrary sign. The constants κ_3 and κ_4 are also positive, indicating the inhibiting nature of v and w. Finally, τ denotes the delay time, whereas the positive parameter α is the delay strength. Note that the time-delayed feedback term is introduced in such a way that the corresponding coupling matrix is a unit one. In the absence of the delayed feedback, the system (1) was first introduced in [26,27] as an extension of the phenomenological model for a planar dc gas-discharge system with high-ohmic semiconductor electrode. Here, the activator u and inhibitor v were interpreted as the current density and voltage drop over the high-ohmic electrode, respectively, whereas the second inhibitor w can be related to the surface charge or other characteristics of the high-ohmic layer [28]. On the other hand, Eq. (1) can be considered as a model system for the investigation of generic features of complex patterns, observed in reaction-diffusion systems, and, e.g., has been already successfully applied to reproduce some of the patterns in the Belousov-Zhabotinsky (BZ) reaction dispersed in a water-in-oil aerosol OT microemulsion [29,30].

Note that reaction-diffusion systems with three and more components arise in a natural way by the description of various chemical, biological, and physical systems [2,11,31]. Especially, three-component reaction-diffusion systems have attracted much attention in recent years. We mention only a three-component Oregonator model, describing photosensitive BZ reaction [32,33], a three-component Gray-Scott model of glycolysis [34], a model for intracellular Ca^{2+} [35], as well as a model of blood clotting [36] or an extended FitzHugh-Nagumo model of *Dictyostelium* amoebae [37].

In addition, in contrast to reaction-diffusion systems with two components, three-component systems allow the theoretical investigation of random set of localized structures that can move and interact with each other [12]. Indeed, a two-component analog of the system (1) (i.e., for $w = 0$) allows solutions in the form of many stationary localized structures in more than one spatial dimension, whereas single moving localized structures can be stabilized by a global feedback term [38]. However, one runs into difficulties if one tries to obtain two or more moving localized structures, as the global feedback does not take account of antisymmetric disturbances [39]. This problem can be easily overcome by introducing of a second inhibiting component, which has to be fast and strongly diffusive and therefore plays the role of a local feedback. In the limit of an infinite diffusion coefficient and for appropriate boundary conditions, the local feedback transforms into the global feedback, making the local feedback approach more general.

II. LINEAR STABILITY ANALYSIS

From now on, we use the general form of the evolution Eq. (1):

$$\partial_t \mathbf{q}(\mathbf{r},t) = \mathfrak{L}[\mathbf{q}(\mathbf{r},t)] + \alpha \, \mathrm{E} \, [\mathbf{q}(\mathbf{r},t) - \mathbf{q}(\mathbf{r},t-\tau)], \tag{2}$$

where $\mathbf{q} = \mathbf{q}(\mathbf{r},t) = [u(\mathbf{r},t), v(\mathbf{r},t), w(\mathbf{r},t)]^T$ is a vector function, $\mathbf{r} \in \mathbb{R}^2$, and $\mathfrak{L}$ is a nonlinear operator

$$\mathfrak{L}[\cdot] = D \nabla^2 + \mathfrak{f}[\cdot].$$

Here, E denotes an identity matrix and the diagonal matrix D contains diffusion constants of the components $u(\mathbf{r},t), v(\mathbf{r},t), w(\mathbf{r},t)$, whereas the vector $\mathfrak{f}[\mathbf{q}(\mathbf{r},t)]$ stands for a nonlinear reaction term.

We are interested in stability of a nontrivial stationary solution $\mathbf{q_0}(\mathbf{r})$ of the system (2), which is shown to exist in appropriate parameter range [40]. The stationary solution exists for all values of the delay strength α and satisfies an equation $\mathfrak{L}[\mathbf{q_0}] = 0$. In the simplest case, it is a stationary localized structure with rotational symmetry. In the absence of the delay term, i.e., for $\alpha = 0$, linear stability of this solution can be analyzed with the aid of the ansatz $\mathbf{q}(\mathbf{r},t) = \mathbf{q_0}(\mathbf{r}) + \boldsymbol{\varphi}(\mathbf{r}) e^{\mu t}$, leading to the linear eigenvalue problem

$$\mathfrak{L}'(\mathbf{q_0})\boldsymbol{\varphi} = \mu \boldsymbol{\varphi}, \tag{3}$$

where the linear operator $\mathfrak{L}'(\mathbf{q_0})$ denotes the linearization of the operator $\mathfrak{L}$ around the stationary solution $\mathbf{q_0}$, μ is the set of eigenvalues of $\mathfrak{L}'(\mathbf{q_0})$, and $\boldsymbol{\varphi}(\mathbf{r})$ are the corresponding eigenfunctions (or modes). As the system (1) features translational invariance with respect to its spatial coordinates, $\mu = 0$ is an eigenvalue of the operator $\mathfrak{L}'(\mathbf{q_0})$, corresponding to two independent neutral eigenfunctions, which we refer to as Goldstone modes. They can be identified as the first derivatives of $\mathbf{q_0}$ with respect to $\mathbf{r}$, i.e., $\boldsymbol{\varphi}^{\mathcal{G}}_{\mathbf{r}} = \partial \mathbf{q_0}/\partial \mathbf{r}$. Notice that continuous spectrum of the operator $\mathfrak{L}'(\mathbf{q_0})$ for the system (1) is separated from zero [41]. That is, only a finite number of eigenfunctions $\propto \boldsymbol{\varphi}_{\mathbf{n}}(\mathbf{r}) e^{in\phi}$, $n \in \mathbb{Z}$, belonging to the discrete spectrum, whose eigenvalues are close to zero can become unstable by the change of some control parameter. Moreover, the operator $\mathfrak{L}'(\mathbf{q_0})$ for the system (1) is not self-adjoint, i.e., these critical discrete eigenfunctions are usually complex. An example of real parts of the u component of first four critical discrete eigenfunctions with positive n is shown in Fig. 1. The influence of the eigenfunctions with different n on the radial-symmetrical localized solution $\mathbf{q_0}$ can be understood as follows: the eigenfunction with $n = 0$, which we refer to as breathing mode [42], results in the change of the size of the localized structure [Fig. 1(a)], the real eigenfunction with $n = 1$ generates the shift of the solution [Fig. 1(b)], whereas $n \geqslant 2$ causes different shape deformations of $\mathbf{q_0}$ [Figs. 1(c) and 1(d)]. Now, we assume that the real parts of all eigenvalues of (3) except for $\mu = 0$ are negative. That is, the stationary solution $\mathbf{q_0}(\mathbf{r})$ for $\alpha = 0$ is stable.

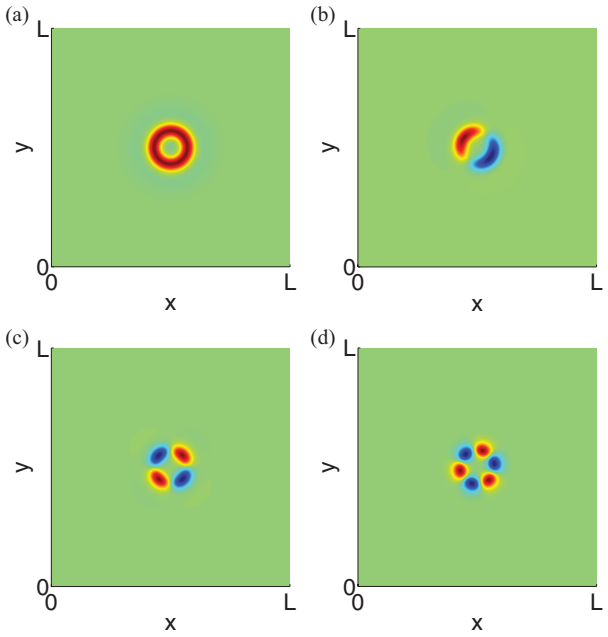

FIG. 1. (Color online) Real parts of the u component of first four critical eigenfunctions with positive n. (a) $n = 0$; (b) $n = 1$; (c) $n = 2$; (d) $n = 3$. Parameters are $D_u = 4.7 \times 10^{-3}$, $D_v = 0$, $D_w = 0.01$, $\lambda = 5.67$, $\kappa_1 = -1.04$, $\kappa_3 = 1.0$, $\kappa_4 = 3.33$, $\eta = 0.7$, $\theta = 0.01$. The calculation was performed on the rectangular domain $[0, L] \times [0, L]$ with $L = 1$ and periodic boundary conditions.

Since the stationary solution is time independent, it is not affected by the delayed feedback term. However, its stability may change. For $\alpha \neq 0$ the linear stability of the system (2) can be determined from the eigenvalue problem

$$\mathfrak{L}'(\mathbf{q_0})\,\boldsymbol{\varphi} = (\lambda - \alpha\,(1 - e^{-\lambda\,\tau}))\,\boldsymbol{\varphi}, \tag{4}$$

where the eigenvalues λ can be found from the transcendental equation [24,25]

$$\mu = \lambda - \alpha\,(1 - e^{-\lambda\,\tau}) \tag{5}$$

as

$$\lambda = \mu + \alpha + \frac{1}{\tau}\,W_m\{-\alpha\tau\,\exp[-(\mu+\alpha)\tau]\}.$$

Here, W_m , $m \in \mathbb{Z}$ is the Lambert W function, defined as the multivalued inverse of the function $z \mapsto z\,e^z$ [43]. Notice that spectra of both linear systems (3), (4) for $\alpha = 0$ and $\alpha \neq 0$ possess the same set of eigenfunctions $\varphi(\mathbf{r})$ as the linearization operator $\mathfrak{L}'(\mathbf{q_0})$ commutes with the identity coupling matrix E.

The stability of the stationary solution $\mathbf{q_0}$ implies that $\mathrm{Re}[\lambda(\mu)] < 0$ for any eigenvalue μ from the spectrum of $\mathfrak{L}'(\mathbf{q_0})$, whereas possible bifurcation points correspond to values of μ, wherein $\mathrm{Re}[\lambda(\mu)]$ vanishes. It can be shown that for all real-valued eigenvalues of μ, the stationary solution of the delayed problem remains stable for $\alpha \leqslant \max\{-\mu/2\,, 1/\tau\}$ [25]. In particular, the neutral eigenvalue $\mu = 0$ yields the bifurcation point $\alpha = 1/\tau$, which corresponds to the onset of spontaneous motion, first observed in the Swift-Hohenberg equation subjected to time-delayed feedback [24]. Indeed, real-valued solutions $\lambda_{1,2}$ of Eq. (5) with $\mu = 0$ are

$$\lambda_1 = 0\,, \quad \lambda_2 \approx -\frac{2}{\tau}\frac{(1-a)}{a},$$

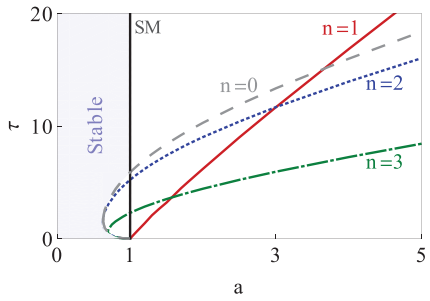

FIG. 2. (Color online) Bifurcation diagram in (a, τ) plane. Different lines represent solutions of Eq. (6) and separate instability regions of eigenfunctions with $n = 0$ (gray dashed curve), $n = 1$ (red solid line), $n = 2$ (blue dotted curve), $n = 3$ (green dashed-dotted curve). Here, each mode is unstable below the corresponding line. The black vertical line $a = 1$ corresponds to the onset of spontaneous motion (SM).

where we introduce a new control parameter $a := \alpha\,\tau$. That is, the system in the presence of the time-delayed feedback remains neutrally stable. However, the eigenvalue λ_2 is negative for $a < 1$ and coincides with λ_1 at $a = 1$. Note that both $\lambda_{1,2}$ correspond to the same neutral eigenfunctions $\boldsymbol{\varphi}^{\mathcal{G}}_{\mathbf{r}}$. For the complex values of μ, the corresponding stability condition for a is much more complicated and can not be written in a compact form. However, the desired instability thresholds for critical eigenfunctions, corresponding to different values of μ can be found by means of the following solvability condition:

$$\pm\arccos(1+x) - \frac{a\,\mathrm{Im}(\mu)}{\mathrm{Re}(\mu)}\,x + 2\pi k = \pm a\,\sqrt{1-(1+x)^2}, \tag{6}$$

where $x = \tau\,a/\mathrm{Re}(\mu)\,, k \in \mathbb{Z}$. Figure 2 shows a bifurcation diagram, collecting the solutions of Eq. (6), obtained for the first four critical modes and for different values of a and τ. The vertical line $a = 1$ corresponds to the onset of spontaneous motion, caused by time-delayed feedback, whereas other lines separate instability regions of eigenfunctions with different n. Here, the critical eigenfunction is unstable below the corresponding line. Note that for $\mathrm{Im}(\mu) \neq 0$, Eq. (6) admits nontrivial solutions for $a < 1$. Hence, complex critical eigenfunctions can become unstable before the spontaneous motion sets in.

The obtained bifurcation diagram clearly indicates the influence of the time-delayed feedback on the stability of the stationary localized solution $\mathbf{q_0}(\mathbf{r})$. Here, different instability scenarios, caused by unstable eigenfunctions with different n can be achieved; the selection of the specific instability type strongly depends on the value of the control parameter a and delay time τ. However, the linear stability analysis is not yet complete, as the time delayed feedback can also influence the stability of the homogeneous steady-state solution $\mathbf{q_h} = (u_h, v_h, w_h)^T$ of the system (2) [25,44]. Indeed, suppose that the steady-state solution $\mathbf{q_h}$ is stable in the absence of the time-delayed feedback, i.e., corresponding growth rates are negative for all values of k. For $\alpha > 0$ the linear stability analysis with respect to perturbations in the form $\propto \exp[i\,k\,\mathbf{r} + \lambda(k)t]$ leads to Eq. (5), where both growth rates μ and λ become now the

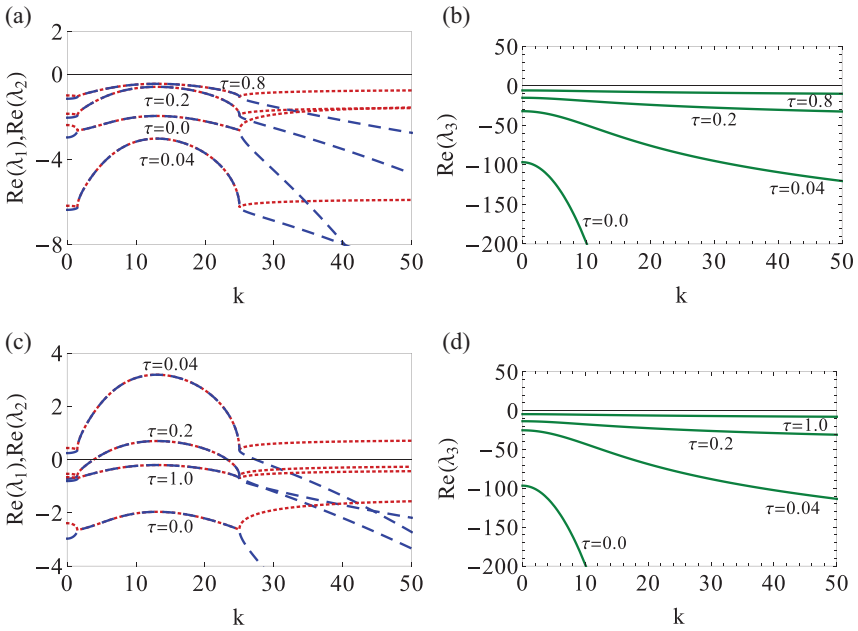

FIG. 3. (Color online) A real part of the growth rates $\lambda_1(k)$, $\lambda_2(k)$ (red dotted and blue dashed-dotted curves, respectively) and $\lambda_3(k)$ (green solid lines), calculated for (a), (b) $a = 0.8$ and (c), (d) $a = 1.05$ for four different values of the delay time τ. Only the main branch of $\mathrm{Re}[\lambda_j(k)]$, $j = \{1, 2, 3\}$, is shown.

functions of the wave number k, i.e.,

$$\mu_j(k) = \lambda_j(k) - \alpha\,(1 - e^{-\lambda_j(k)\tau}), \quad j = \{1, 2, 3\}.$$

As before, the complex solutions of this equation can be found in the form of the Lambert W function, and depend on both control parameters a and τ. The dependence of $\mathrm{Re}[\lambda_j(k)]$ on the delay time τ, calculated for two fixed values of $a = 0.8$ and 1.05, is presented in Fig. 3. Only the main branch of the solution, corresponding to the Lambert function W_0, is shown as other branches are situated far away from zero for rather small values of a and τ. One can see that for $\tau = 0$, all $\mathrm{Re}[\lambda_j(k)] < 0$ for any k, i.e., the homogeneous solution is stable. For $\tau > 0$, the behavior of $\mathrm{Re}[\lambda_j(k)]$ depends on the value of the control parameter a: While for $a < 1$ the sign of the real part of all $\lambda_j(k)$ remains negative for all values of τ [see Figs. 3(a)and 3(b)], for $a > 1$ $\mathrm{Re}[\lambda_{1,2}(k)]$ becomes positive for some τ, indicating the existence of the traveling wave bifurcation with a finite wave number $k = k_c$ [25,44], whereas $\mathrm{Re}[\lambda_3(k)]$ keeps the negative sign [Fig. 3(d)]. Indeed, for rather small values of τ [see Fig. 3(c) for $\tau = 0.04$] $\mathrm{Re}[\lambda_1(k)] > 0$ for all k, whereas the band of unstable modes becomes finite for both $\mathrm{Re}[\lambda_{1,2}(k)]$ with increase in τ [Fig. 3(c) for $\tau = 0.2$]. Further increase in τ leads to the stabilization of the homogeneous solution $\mathbf{q_h}$ [see Fig. 3(c) for $\tau = 1.0$]. That is, the time-delayed feedback influences the stability properties of the homogeneous steady-state solution only for small delay times. Note that the instability threshold of the traveling wave bifurcation for different values of a and τ can also be found within the solvability condition (6).

III. DIRECT NUMERICAL SIMULATIONS

As is shown above, solutions of Eq. (6) allow effective control of the instability type. In particular, for rather small delay times, different critical eigenfunctions are unstable simultaneously if one changes control parameters a and τ. In addition, the homogeneous solution can be unstable as well, that is, the dynamical behavior of the system in this parameter region can be very complex. An example of such a complex behavior is illustrated in Fig. 4, where the time evolution of the localized solution of Eq. (1), calculated for $a = 1.05$ and $\tau = 0.2$, is presented. Numerical simulations have been performed on the two-dimensional square domain $[-L, L] \times [-L, L]$ with periodic boundary conditions using a pseudospectral method with 512×512 grid points, whereas a Runge-Kutta 4 scheme is employed for the time stepping. In this parameter range, apart from unstable spatial

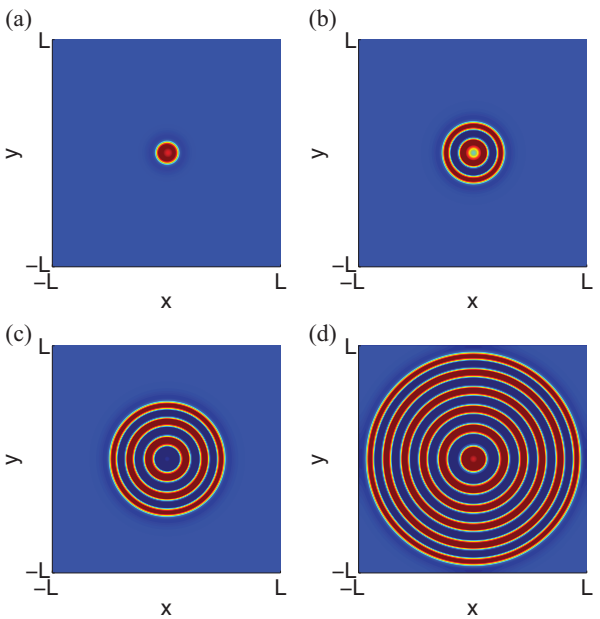

FIG. 4. (Color online) Numerical solution of Eq. (1), obtained for $a = 1.05$, $\tau = 0.2$ for four different time moments (a) $t = 90$; (b) $t = 180$; (c) $t = 300$; (d) $t = 420$, showing the formation of a target pattern. Activator distribution is shown. Numerical simulations have been performed on the two-dimensional square domain $[-L, L] \times [-L, L]$, $L = 2$ with periodic boundary conditions. Other parameters are the same as in Fig. 1.

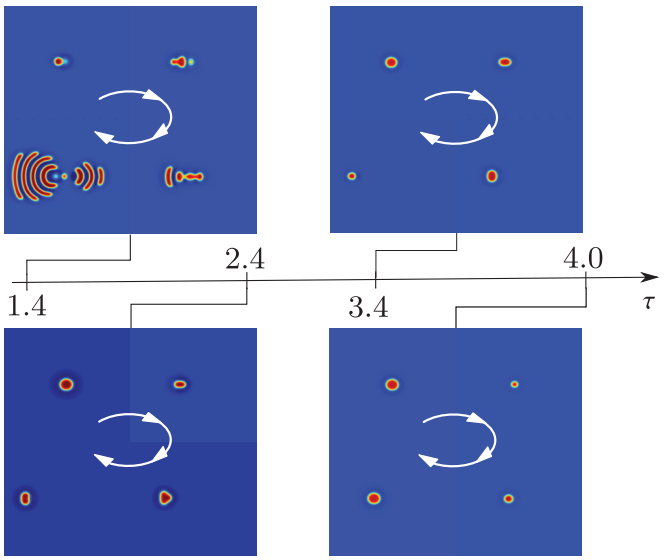

FIG. 5. (Color online) Time evolution of the activator distribution obtained from numerical solution of Eq. (1) for $a = 1.05$ and four different delay times $\tau = \{1.4, 2.4, 3.4, 4.0\}$. Parameters are the same as in Figs. 1 and 4. White arrows indicate the direction of the time evolution.

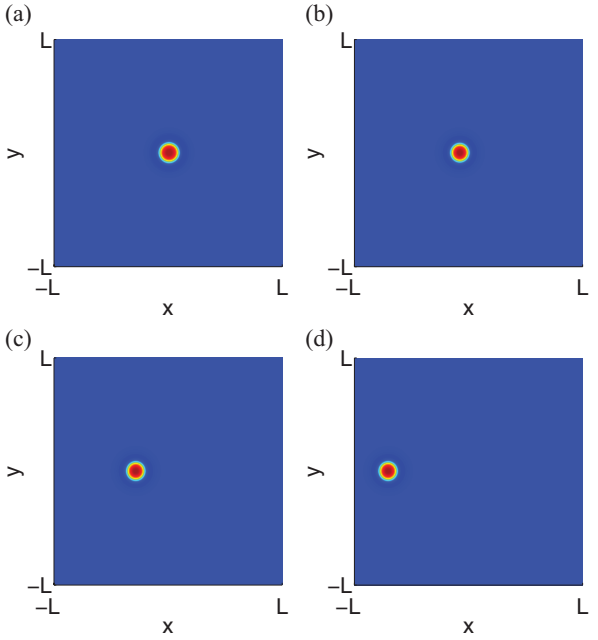

FIG. 6. (Color online) An example of a delayed-induced motion of the localized structure, obtained by numerical simulation of the model Eq. (1) at $a = 1.6$, $\tau = 12$ for four different time moments: (a) $t = 120$; (b) $t = 600$; (c) $t = 1200$; (d) $t = 2000$.

eigenfunctions, the traveling wave bifurcation of the homogeneous solution $\mathbf{q_h}$ takes place [see also Fig. 3(c)]. Here, the localized initial condition breaks in a periodically repeating sequence in which the center of the pattern oscillates while the individual rings propagate from the center to the boundary, i.e., a target pattern arises. If the delay time τ is increased for a fixed value of the control parameter a, $\mathbf{q_h}$ becomes stable and only unstable spatial eigenfunctions influence the behavior of the localized structure. This situation is illustrated in Fig. 5, where numerical solutions of Eq. (1), calculated for four different delay times τ, keeping the value of the control parameter $a = 1.05$ fixed, are shown. As $a > 1$, spontaneous motion takes place and impacts on the dynamics of the solution. For delay times, chosen relatively close to the threshold of the traveling wave bifurcation (see Fig. 5 for $\tau = 1.4$), the localized initial pulse starts to move and oscillate because of the breathing mode with $n = 0$. Here, the real eigenfunction with $n = 1$ breaks the symmetry, so that the localized structure becomes unsymmetrical, whereas the complex eigenfunction with $n = \pm 2, \pm 3$ with large imaginary parts contributes to the shape deformation. As a result, a new pulse is formed from the right tail of the initial structure. This new pulse is also unstable, i.e., a further pulse is generated from the second one. The newly formed pulses propagate from the center to the domain boundary and finally a complex pattern, consisting of wave segment trains, arises. As τ increases, the mode $n = 1$ becomes stable and at the same time frequencies, corresponding to complex unstable eigenfunctions, diminish, which provides a way to obtain solutions of Eq. (1) with bounded shape configuration. Such an example is shown in Fig. 5 for $\tau = 2.4$. Here, all unstable complex eigenfunctions with $|n| \leqslant 3$ influence the dynamics of the initial localized structure: It moves with a constant velocity and oscillates with a constant amplitude ($n = 0$), whereas its shape deforms according to the action of modes $n = \pm 2, \pm 3$. A similar scenario is obtained for $\tau = 3.4$, which value is already above the threshold for $n = 3$. Here, a resulting localized structure also moves and breathes, whereas the shape deformation is governed only by modes with $n = \pm 2$. If one increases the delay time τ further, the modes with $n = \pm 2$ become damped too, and the time dynamics is mostly governed by the breathing mode $n = 0$, i.e., a moving and breathing localized structure arises (see Fig. 5 for $\tau = 4$). Note that moving and breathing localized structures can be found in reaction-diffusion systems without time-delayed feedback [45], in contrast to previous stable configurations, where several complex modes with $n > 0$ are unstable simultaneously.

As the bifurcation diagram indicates (see Fig. 2), further increase in τ leads to stabilization of all critical modes with different n and only spontaneous motion of the localized structure, induced by the time-delayed feedback, defines the behavior of the solution. This situation is shown in Fig. 6, where numerical solution, obtained for $a = 1.6$ and $\tau = 12$, is presented. Here, the localized structure moves with a constant velocity without pronounced change in its shape (see also [24,25,44], where the case of the delayed-induced spontaneous motion of the localized structures in the Swift-Hohenberg equation was discussed in detail).

IV. ORDER PARAMETER EQUATION

Linear stability analysis supported by direct numerical simulations of Eq. (1) shows that the presence of the time-delayed feedback leads to a complex dynamical behavior of the corresponding solutions, making the full bifurcation analysis of the problem very complicated and practically impossible. A bifurcation analysis of the localized structure in the Swift-Hohenberg equation with the time-delayed feedback

was performed in [25] and a system of order parameter equations, explicitly describing the temporal evolution of the localized structure in the vicinity of the bifurcation point was derived. However, for the reaction-diffusion system (1) we are interested in, the spectrum of the linear problem is complex, making mathematical treatment here much more complicated. Nevertheless, one can try to understand at least a rather simple bifurcation scenario, corresponding to the case of spontaneous motion in order to understand how the delay term impacts on the dynamics of the moving localized structure.

An instability of the stationary solution $\mathbf{q_0}$ is characterized by the eigenvalues of the corresponding linear eigenvalue problem. That is, if we are interested in an evolution of a small perturbation $\mathbf{w}(\mathbf{r},t)$, so that $\mathbf{q} = \mathbf{q_0} + \mathbf{w}(\mathbf{r},t)$, it is convenient to perform a normal mode ansatz. In addition, as the system (1) possesses translational symmetry, each solution $\mathbf{q}(\mathbf{r},t)$ remains a solution if it is shifted to a different spatial position, given by the constant vector $\mathbf{R}$. That is, e.g., at the bifurcation point $a = 1$

$$\mathbf{q}(\mathbf{r},t) = \mathbf{q_0}(\mathbf{r} - \mathbf{R}) + \mathbf{w}(\mathbf{r} - \mathbf{R}, t),$$

where $\mathbf{w}(\mathbf{x},\mathbf{t}) = \sum_j \boldsymbol{\varphi}_j(\mathbf{r})\, e^{\lambda_j t}$ is a sum of all stable modes of the delayed problem and the neutral modes $\boldsymbol{\varphi}_{\mathbf{r}}^{\mathcal{G}}$ are incorporated into the shifted stationary solution, as an infinitesimal shift corresponds to an addition of the spatial derivative of the solution in the respective direction, i.e., the Goldstone mode. On the other hand, translational symmetry is characterized by its infinitesimal generators $\mathbf{g} = \frac{1}{i}\nabla$ and is of the form $D(\mathbf{R}) = e^{i\,\mathbf{R}\cdot\mathbf{g}}$ [46,47]. That is, one can rewrite the last equation as

$$\mathbf{q}(\mathbf{r},t) = e^{-\mathbf{R}\cdot\nabla}\,(\mathbf{q_0}(\mathbf{r}) + \mathbf{w}(\mathbf{r}, t)).$$

Note that the spontaneous motion is caused only by the neutral Goldstone modes $\boldsymbol{\varphi}_{\mathbf{r}}^{\mathcal{G}}$; all other critical modes are stable. Hence, if we increase the control parameter a, $a = 1 + \varepsilon$, $\varepsilon \ll 1$, and let the time delay τ be in the parameter range, where only delayed-induced drift instability determines the time evolution of the system, the neutral Goldstone modes begin to be active and the vector $\mathbf{R}$, describing the shift of the pattern becomes a slow function of time. That is, we can perform the following ansatz in the vicinity of the bifurcation point $a = 1$ [25,46,47]:

$$\begin{aligned}\mathbf{q}(\mathbf{r},t) &= \mathbf{q_0}[\mathbf{r} - \mathbf{R}(t)] + \mathbf{w}[\mathbf{r} - \mathbf{R}(t), t]\\ &= e^{-\mathbf{R}(t)\cdot\nabla}\,(\mathbf{q_0}(\mathbf{r}) + \mathbf{w}(\mathbf{r}, t)).\end{aligned} \tag{7}$$

From the point of view of group theoretic methods, this symmetry breaking instability induces a motion along the group orbit, given by $D[\mathbf{R}(t)]\,\mathbf{q_0}$. Here, $\mathbf{R}(t)$ induces a drift of the localized solution [47].

Inserting the ansatz (7) into the basic evolution equation (2) we obtain

$$\begin{aligned}&-\dot{\mathbf{R}}(t)\,[\nabla\mathbf{q_0}(\mathbf{r}) + \nabla\mathbf{w}(\mathbf{r}, t)] + \frac{\partial\mathbf{w}(\mathbf{r}, t)}{\partial t}\\ &\quad= \mathfrak{L}'(\mathbf{q_0})\mathbf{w}(\mathbf{r}, t) + \mathbf{N}[\mathbf{w}(\mathbf{r}, t)] + \alpha\,\mathbf{M}[\mathbf{r}, \mathbf{R}(t) - \mathbf{R}(t-\tau),\\ &\qquad\times \mathbf{w}(\mathbf{r}, t), \mathbf{w}(\mathbf{r}, t-\tau)].\end{aligned} \tag{8}$$

Here,

$$\mathbf{N}[\mathbf{w}(\mathbf{r}, t)] = \frac{1}{2!}\,\mathfrak{L}''(\mathbf{q_0})\mathbf{w}:\mathbf{w} + \frac{1}{3!}\,\mathfrak{L}'''(\mathbf{q_0})\mathbf{w}:\mathbf{w}:\mathbf{w}$$

contains nonlinear contributions up to third order and delay terms are lumped into

$$\begin{aligned}&\mathbf{M}[\mathbf{r}, \mathbf{R}(t) - \mathbf{R}(t-\tau), \mathbf{w}(\mathbf{r}, t), \mathbf{w}(\mathbf{r}, t-\tau)]\\ &\quad= \mathbf{w}(\mathbf{r}, t) - \mathbf{w}(\mathbf{r}, t-\tau) + (1 - e^{(\mathbf{R}_t - \mathbf{R}_{t-\tau})\cdot\nabla})\\ &\qquad\times[\mathbf{q_0}(\mathbf{r}) + \mathbf{w}(\mathbf{r}, t-\tau)].\end{aligned}$$

The notation used in $\mathbf{N}[\mathbf{w}(\mathbf{r}, t)]$ is a shorthand notation: In general, quadratic and cubic terms are functionals quadratic and cubic in $\mathbf{w}(\mathbf{r}, t)$, whereas $\mathfrak{L}^{(n)}(\mathbf{q_0})$ denotes the nth Fréchet derivative with respect to $\mathbf{q}$, calculated at $\mathbf{q} = \mathbf{q_0}$.

In the following, we shall decompose this equation in such a way that we obtain an evolution equation for the shift $\mathbf{R}(t)$ as well as an evolution equation for the change of the shape of the localized structure in terms of the deformation $\mathbf{w}(\mathbf{r}, t)$. An equation for the shift $\mathbf{R}(t)$ is obtained by requiring that the shape deformation is orthogonal to the adjoint Goldstone mode $\boldsymbol{\varphi}_{\mathbf{r}}^{\mathcal{G}\dagger}$, defined as a neutral eigenfunction of the adjoint linear operator $\mathfrak{L}'^{\dagger}(\mathbf{q_0})$. This condition leads to

$$\begin{aligned}&-\dot{\mathbf{R}}(t)\left(\left\langle\boldsymbol{\varphi}_{\mathbf{r}}^{\mathcal{G}\dagger}\middle|\boldsymbol{\varphi}_{\mathbf{r}}^{\mathcal{G}}\right\rangle - \left\langle\nabla\boldsymbol{\varphi}_{\mathbf{r}}^{\mathcal{G}\dagger}\middle|\mathbf{w}(\mathbf{r}, t)\right\rangle\right)\\ &\quad= \alpha\left\langle\boldsymbol{\varphi}_{\mathbf{r}}^{\mathcal{G}\dagger}\middle|\mathbf{N}[\mathbf{w}(\mathbf{r}, t)]\right\rangle - \alpha\,[\mathbf{R}(t) - \mathbf{R}(t-\tau)]\left\langle\boldsymbol{\varphi}_{\mathbf{r}}^{\mathcal{G}\dagger}\middle|\boldsymbol{\varphi}_{\mathbf{r}}^{\mathcal{G}}\right\rangle\\ &\qquad+\alpha\,[\mathbf{R}(t) - \mathbf{R}(t-\tau)]\left\langle\boldsymbol{\varphi}_{\mathbf{r}}^{\mathcal{G}\dagger}\middle|\nabla\mathbf{w}(\mathbf{r}, t-\tau)\right\rangle\\ &\qquad-\frac{\alpha}{6}\,|\mathbf{R}(t) - \mathbf{R}(t-\tau)|^2\,[\mathbf{R}(t) - \mathbf{R}(t-\tau)]\left\langle\boldsymbol{\varphi}_{\mathbf{r}}^{\mathcal{G}\dagger}\middle|\nabla\nabla\boldsymbol{\varphi}_{\mathbf{r}}^{\mathcal{G}}\right\rangle.\end{aligned} \tag{9}$$

Here, $\langle\ldots|\ldots\rangle$ denotes the scalar product defined in terms of full spatial integration over the considered domain and we used the expansion

$$\begin{aligned}&1 - e^{[\mathbf{R}(t) - \mathbf{R}(t-\tau)]\cdot\nabla}\\ &\quad= -[\mathbf{R}(t) - \mathbf{R}(t-\tau)]\cdot\nabla - \frac{1}{2!}\,\{[\mathbf{R}(t) - \mathbf{R}(t-\tau)]\cdot\nabla\}^2\\ &\qquad-\frac{1}{3!}\,\{[\mathbf{R}(t) - \mathbf{R}(t-\tau)]\cdot\nabla\}^3.\end{aligned}$$

The evolution equation for the shape deformation $\mathbf{w}(\mathbf{r}, t)$ is obtained by substituting the evolution equation (9) into Eq. (8). As a consequence, the equation for $\mathbf{w}(\mathbf{r}, t)$ to the lowest order reads as

$$\begin{aligned}\frac{\partial\mathbf{w}(\mathbf{r}, t)}{\partial t} &= \mathfrak{L}'(\mathbf{q_0})\mathbf{w}(\mathbf{r}, t) + \alpha[\mathbf{w}(\mathbf{r}, t) - \mathbf{w}(\mathbf{r}, t-\tau)]\\ &\quad-\frac{\alpha}{2}\,\{[\mathbf{R}(t) - \mathbf{R}(t-\tau)]\cdot\nabla\}^2\,\mathbf{q_0}(\mathbf{r}).\end{aligned} \tag{10}$$

As already mentioned above, we suppose that all critical modes except for the neutral ones are stable. That is, as a first approximation we can look for stationary states of the shape deformation, applying the adiabatic approximation $\partial\mathbf{w}(\mathbf{r}, t)/\partial t \approx 0$, yielding

$$\mathfrak{L}'(\mathbf{q_0})\mathbf{w}(\mathbf{r}, t) = \frac{\alpha}{2}\,\{[\mathbf{R}(t) - \mathbf{R}(t-\tau)]\cdot\nabla\}^2\,\mathbf{q_0}(\mathbf{r}).$$

Hence, one can calculate the shape deformation $\mathbf{w}(\mathbf{r}, t)$ as

$$\mathbf{w}(\mathbf{r}, t) = [\mathfrak{L}'(\mathbf{q_0})]^{-1}\left[\frac{\alpha}{2}\,\{[\mathbf{R}(t) - \mathbf{R}(t-\tau)]\cdot\nabla\}^2\,\mathbf{q_0}(\mathbf{r})\right]. \tag{11}$$

Substituting this relation into the evolution equation (9) for the shift $\mathbf{R}(t)$, to the lowest order, we obtain

$$\dot{\mathbf{R}}(t) = \alpha\,[\mathbf{R}(t) - \mathbf{R}(t-\tau)] - \frac{\alpha}{6}\,\frac{\langle \nabla\boldsymbol{\varphi}_{\mathbf{r}}^{\mathcal{G}\dagger}|\nabla\boldsymbol{\varphi}_{\mathbf{r}}^{\mathcal{G}}\rangle}{\langle \boldsymbol{\varphi}_{\mathbf{r}}^{\mathcal{G}\dagger}|\boldsymbol{\varphi}_{\mathbf{r}}^{\mathcal{G}}\rangle}\,|\mathbf{R}(t) - \mathbf{R}(t-\tau)|^2[\mathbf{R}(t) - \mathbf{R}(t-\tau)]. \tag{12}$$

A nonlinear delay differential equation (12) is an order parameter equation, describing the behavior of the localized structure in the vicinity of the bifurcation point $a = 1$. Note that nonlinear terms in $\mathbf{w}(\mathbf{r}, t)$, contained in $\mathbf{N}[\mathbf{w}(\mathbf{r}, t)]$, are higher-order terms, i.e., spontaneous motion to the lowest order occurs without change of the shape of the localized structure.

In order to derive the time evolution of the drift velocity $\mathbf{V}(t) = \dot{\mathbf{R}}(t)$ of the moving localized solution near the bifurcation point $a = 1$, i.e., for $a = 1 + \varepsilon$, $\varepsilon \ll 1$, the following expansion is performed:

$$\mathbf{R}(t-\tau) = \mathbf{R}(t) - \tau\,\mathbf{V}(t) + \frac{\tau^2}{2}\dot{\mathbf{V}}(t) + \mathcal{O}(\ddot{\mathbf{V}}(t)),$$

as the position $\mathbf{R}(t)$ and consequently the velocity $\mathbf{V}(t)$ are slowly varying quantities in time in the vicinity of $a = 1$. Substitution of this relation into order parameter (12) yields

$$\dot{\mathbf{R}}(t) = \mathbf{V}(t),$$
$$\frac{a\,\tau}{2}\dot{\mathbf{V}}(t) = (a-1)\mathbf{V}(t) - \frac{a\,\tau^2}{6}\,\frac{\langle \nabla\boldsymbol{\varphi}_{\mathbf{r}}^{\mathcal{G}\dagger}|\nabla\boldsymbol{\varphi}_{\mathbf{r}}^{\mathcal{G}}\rangle}{\langle \boldsymbol{\varphi}_{\mathbf{r}}^{\mathcal{G}\dagger}|\boldsymbol{\varphi}_{\mathbf{r}}^{\mathcal{G}}\rangle}\,|\mathbf{V}(t)|^2\,\mathbf{V}(t), \tag{13}$$

which can be recognized as a pitchfork normal form of the delayed-induced drift bifurcation [25] and essentially coincides with the normal form of a classical drift bifurcation [11,48]. Note that Eq. (13) represents a generalization of the normal form of the delayed-induced drift bifurcation, derived in [25] for the Swift-Hohenberg equation, to the case of systems with complex spectra. That is, the corresponding normal form for systems with self-adjoint linearization operators (e.g., for the Swift-Hohenberg equation) can be directly obtained from the system (13) having applied $\boldsymbol{\varphi}_{\mathbf{r}}^{\mathcal{G}\dagger} = \boldsymbol{\varphi}_{\mathbf{r}}^{\mathcal{G}}$.

Equation (13) has a trivial stationary solution $V = 0$, which is stable for $a \leqslant 1$. For $a > 1$, one can also find the nontrivial stable stationary drift velocity

$$V = \pm\frac{1}{\tau}\sqrt{\frac{6\,(a-1)}{\beta\,a}}, \tag{14}$$

where $\beta = \frac{\langle \nabla\boldsymbol{\varphi}_{\mathbf{r}}^{\mathcal{G}\dagger}|\nabla\boldsymbol{\varphi}_{\mathbf{r}}^{\mathcal{G}}\rangle}{\langle \boldsymbol{\varphi}_{\mathbf{r}}^{\mathcal{G}\dagger}|\boldsymbol{\varphi}_{\mathbf{r}}^{\mathcal{G}}\rangle}$. One can see that the drift velocity (14) is a function of the control parameter a and delay time τ and depends on the constant coefficient β. Note that the drift velocity has the same functional dependence on the distance to the bifurcation point and on the shape factor β as the velocity of the moving localized structure if the drift bifurcation takes place [11,48] and differs from it in the a and τ dependencies. Let us remark here that the stable stationary drift velocity V can be also calculated directly from the order parameter equation (12). Indeed, looking here for solutions, traveling with the constant velocity V one gets

$$1 = \alpha\,\tau - \frac{\alpha\,\beta\,\tau^3}{6}\,V^2.$$

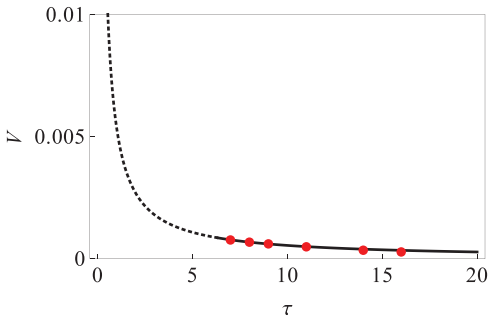

FIG. 7. (Color online) Analytical prediction of the velocity of the localized structure (black line) calculated from Eq. (14) for fixed value of the control parameter $a = 1.05$, compared with direct numerical simulations (red circles). Black dotted line indicates the parameter range where other critical modes with different n are unstable. Parameters are the same as in Figs. 1 and 4.

Solving this equation for V, one immediately obtains the same expression (14) for the stationary drift velocity. That is to say that approximation we used to derive the normal form (13) works well in the vicinity of the bifurcation point $a = 1$.

In order to calculate the constant drift velocity (14), one needs the explicit expression for the coefficient $\boldsymbol{\varphi}_{\mathbf{r}}^{\mathcal{G}\dagger}$. Note that in general the analytical calculation of the eigenfunctions $\boldsymbol{\varphi}_{\mathbf{r}}^{\mathcal{G}\dagger}$ of the adjoint operator $\mathfrak{L}'^{\dagger}(\mathbf{q_0})$ is difficult, but in the case of the reaction-diffusion system (1) it is possible using the relation [49,50]

$$\boldsymbol{\varphi}_{\mathbf{r}}^{\mathcal{G}\dagger} = M^{-1}\,\boldsymbol{\varphi}_{\mathbf{r}}^{\mathcal{G}},$$

where M is a diagonal matrix, defined as

$$M = \begin{pmatrix} 1 & 0 & 0 \\ 0 & -\frac{1}{\kappa_3\,\eta} & 0 \\ 0 & 0 & -\frac{1}{\kappa_4\theta} \end{pmatrix}.$$

That is, the coefficient β can be directly calculated from the shape of the stationary localized solution $\mathbf{q_0}(\mathbf{r})$. Now, we are in a good position to calculate the drift velocity of the localized structure given by Eq. (14) and compare the predictions with direct numerical simulations of the system (1). The result of this comparison is shown in Fig. 7, where the dependence of the velocity V on the delay time τ is calculated both analytically and numerically, keeping the value of a fixed. A dotted line corresponds to the parameter range, where eigenfunctions with different n are unstable (compare with bifurcation diagram, shown in Fig. 2).

V. CONCLUSION

In this paper, stability properties of a single localized structure in a three-component reaction-diffusion system subjected to the time-delayed feedback were investigated in detail. It was shown that the presence of the time-delayed term results in nontrivial instabilities of the localized structure, leading to the formation of complex spatial-temporal structures such as target patterns, moving and breathing objects, as well as various structures resulting from multimode oscillatory instabilities. The instability scenarios can be fully analyzed in terms of the spectrum of the linear problem of the reaction-diffusion system without time-delayed feedback and bifurcation

diagram, possessing information about instability thresholds can be achieved. The bifurcation diagram indicates that variation in the product of the delay time and delay strength allows the control of the instability type in a straightforward manner.

In addition, a bifurcation scenario, corresponding to the case of spontaneous motion, was investigated in order to understand how the delay term impacts on the dynamics of the moving localized structure. As a result, an order parameter equation for the position of the localized structure was derived, whereas the corresponding evolution equation for the deformation of the shape of the localized structure was excluded adiabatically. The desired order parameter equation is a subject to a nonlinear delay-differential equation, explicitly describing its temporal evolution in the vicinity of the bifurcation point, which can be transformed to the normal form of the pitchfork drift bifurcation.

The information about the system behavior is now contained in the real coefficients of this equation. The latter are the functions of the stationary solution and neutral eigenfunctions and can be directly calculated from the original reaction-diffusion system in question. Comparison of the results with direct numerical simulations of the full system shows that both approaches are in good agreement. To conclude, note that all results are derived in general form and go beyond reaction-diffusion systems. That is, the presented formalism can be applied to a wide class of spatial extended systems with both real and complex spectra.

ACKNOWLEDGMENT

We gratefully acknowledge many fruitful discussions with the late Professor Rudolf Friedrich.

[1] *Handbook of Chaos Control*, 2nd ed., edited by E. Schöll and H. G. Schuster (Wiley-VCH, Weinheim, 2008).
[2] A. S. Mikhailov and K. Showalter, Phys. Rep. **425**, 79 (2006).
[3] K. Pyragas and A. Tamaševičius, Phys. Lett. A **180**, 99 (1993).
[4] O. Lüthje, S. Wolff, and G. Pfister, Phys. Rev. Lett. **86**, 1745 (2001).
[5] J. Schlesner, A. Amann, N. B. Janson, W. Just, and E. Schöll, Phys. Rev. E **68**, 066208 (2003).
[6] K. A. Montgomery and M. Silber, Nonlinearity **17**, 2225 (2004).
[7] C. M. Postlethwaite and M. Silber, Phys. D (Amsterdam) **236**, 65 (2007).
[8] M. Kehrt, P. Hövel, V. Flunkert, M. A. Dahlem, P. Rodin, and E. Schöll, Eur. Phys. J. B **68**, 557 (2009).
[9] Y. N. Kyrychko, K. B. Blyuss, S. J. Hogan, and E. Schöll, Chaos **19**, 043126 (2009).
[10] *Dissipative Solitons: From Optics to Biology and Medicine*, edited by A. Ankiewicz and N. Akhmediev, Lecture Notes in Physics, Vol. 751 (Springer, Berlin, 2008).
[11] H.-G. Purwins, H. U. Bödeker, and S. Amiranashvili, Adv. Phys. **59**, 485 (2010).
[12] A. W. Liehr, *Dissipative Solitons in Reaction Diffusion Systems. Mechanism, Dynamics, Interaction*, Springer Series in Synergetics, Vol. 70 (Springer, Berlin, 2013).
[13] C. Christov and M. Velarde, Phys. D (Amsterdam) **86**, 323 (1995).
[14] B. S. Kerner and V. V. Osipov, *Autosolitons. A New Approach to Problems of Self-Organization and Turbulence*, Fundamental Theories of Physics, Vol. 61 (Kluwer Academic, Dordrecht, 1994).
[15] O. Lioubashevski, Y. Hamiel, A. Agnon, Z. Reches, and J. Fineberg, Phys. Rev. Lett. **83**, 3190 (1999).
[16] J. Fort and V. Méndez, Phys. Rev. Lett. **89**, 178101 (2002).
[17] V. Ortega-Cejas, J. Fort, and V. Méndez, Ecology **85**, 258 (2004).
[18] M. A. Dahlem, F. M. Schneider, and E. Schöll, Chaos **18**, 026110 (2008).
[19] F. Schneider, E. Schöll, and M. Dahlem, Chaos **19**, 015110 (2009).
[20] M. A. Dahlem, R. Graf, A. J. Strong, J. P. Dreier, Y. A. Dahlem, M. Sieber, W. Hanke, K. Podoll, and E. Schöll, Phys. D (Amsterdam) **239**, 889 (2010).
[21] T. Erneux, G. Kozyreff, and M. Tlidi, Philos. Trans. R. Soc. London, Ser. A **368**, 483 (2010).
[22] P. V. Paulau, D. Gomila, T. Ackemann, N. A. Loiko, and W. J. Firth, Phys. Rev. E **78**, 016212 (2008).
[23] Y. Tanguy, N. Radwell, T. Ackemann, and R. Jäger, Phys. Rev. A **78**, 023810 (2008).
[24] M. Tlidi, A. G. Vladimirov, D. Pieroux, and D. Turaev, Phys. Rev. Lett. **103**, 103904 (2009).
[25] S. V. Gurevich and R. Friedrich, Phys. Rev. Lett. **110**, 014101 (2013).
[26] R. Woesler, P. Schütz, M. Bode, M. Or-Guil, and H.-G. Purwins, Phys. D (Amsterdam) **91**, 376 (1996).
[27] C. P. Schenk, M. Or-Guil, M. Bode, and H.-G. Purwins, Phys. Rev. Lett. **78**, 3781 (1997).
[28] E. L. Gurevich, A. W. Liehr, S. Amiranashvili, and H.-G. Purwins, Phys. Rev. E **69**, 036211 (2004).
[29] A. A. Cherkashin, V. K. Vanag, and I. R. Epstein, J. Chem. Phys. **128**, 204508 (2008).
[30] S. Alonso, K. John, and M. Bär, J. Chem. Phys. **134**, 094117 (2011).
[31] V. K. Vanag and I. R. Epstein, Chaos **17**, 037110 (2007).
[32] T. Amemiya, P. Kettunen, S. Kadar, T. Yamaguchi, and K. Showalter, Chaos **8**, 872 (1998).
[33] G. Bordiougov and H. Engel, Phys. Rev. Lett. **90**, 148302 (2003).
[34] Y. Nishiura, T. Teramoto, and K.-I. Ueda, Chaos **15**, 047509 (2005).
[35] M. Falcke, M. Or-Guil, and M. Bär, Phys. Rev. Lett. **84**, 4753 (2000).
[36] E. S. Lobanova and F. I. Ataullakhanov, Phys. Rev. Lett. **91**, 138301 (2003).
[37] I. Aranson, H. Levine, and L. Tsimring, Phys. Rev. Lett. **76**, 1170 (1996).
[38] K. Krischer and A. Mikhailov, Phys. Rev. Lett. **73**, 3165 (1994).
[39] L. Schimansky-Geier, C. Zülicke, and E. Schöll, Z. Phys. B **84**, 433 (1991).
[40] P. Heijster and B. Sandstede, J. Nonlinear Sci. **21**, 705 (2011).
[41] T. Kato, *Perturbation Theory for Linear Operators* (Springer, Berlin, 1966).

[42] S. V. Gurevich, S. Amiranashvili, and H.-G. Purwins, Phys. Rev. E **74**, 066201 (2006).
[43] R. M. Corless, G. H. Gonnet, D. E. G. Hare, D. J. Jeffrey, and D. E. Knuth, Adv. Comput. Math. **5**, 329 (1996).
[44] M. Tlidi, A. G. Vladimirov, D. Turaev, G. Kozyreff, D. Pieroux, and T. Erneux, Eur. Phys. J. D **59**, 59 (2010).
[45] S. V. Gurevich and R. Friedrich (unpublished).
[46] R. Friedrich, Z. Phys. B **90**, 373 (1993).
[47] R. Friedrich, in *Collective Dynamics of Nonlinear and Disordered Systems*, edited by G. Radons, W. Just, and P. Häussler (Springer, Berlin, 2005), pp. 61–84.
[48] M. Or-Guil, M. Bode, C. P. Schenk, and H.-G. Purwins, Phys. Rev. E **57**, 6432 (1998).
[49] A. S. Moskalenko, A. W. Liehr, and H.-G. Purwins, Europhys. Lett. **63**, 361 (2003).
[50] S. V. Gurevich, H. U. Bödeker, A. S. Moskalenko, A. W. Liehr, and H.-G. Purwins, Phys. D (Amsterdam) **199**, 115 (2004).